This is not a peer-reviewed article.
5th National Decennial Irrigation CD-ROM Proceedings
Phoenix Convention Center, 5 - 8 December 2010, Phoenix, AZ USA
M. Dukes ed. St Joseph Mich: ASABE
ASABE Publication Number 711P0810cd

2950 Niles Road, St. Joseph, MI 49085-9659, USA
269.429.0300 fax 269.429.3852 hq@asabe.org www.asabe.org

An ASABE Conference Presentation

Paper Number: IRR10-9971

Status and continuing challenges in operational remote sensing of ET

Richard G. Allen

University of Idaho, 3793 N 3600 E, Kimberly, ID 83341, USA, rallen@kimberly.uidaho.edu

Jan Hendrickx

Dept. Earth and Environmental Science, MSEC 240, New Mexico Tech, Socorro, NM 87801, USA, janhendrickxnmt@gmail.com

Wim Bastiaanssen

WaterWatch, Generaal Foulkesweg 28a, 6703 BS Wageningen, Netherlands 0317 423401, w.bastiaanssen@waterwatch.nl

Jeppe Kjaersgaard

University of Idaho, 3793 N 3600 E, Kimberly, ID, 83341, USA, jeppek@kimberly.uidaho.edu

Ayse Irmak

School of Natural Resources University of Nebraska–Lincoln, 311 HARH, Lincoln NE 68583-0973, USA, airmak2@unlnotes.unl.edu

Justin Huntington

Desert Research Institute, 2215 Raggio Parkway, Reno, NV 89512, USA, Justin.Huntington@dri.edu

Written for presentation at the
5th National Decennial Irrigation Conference
Sponsored jointly by ASABE and the Irrigation Association
Phoenix Convention Center
Phoenix, Arizona
December 5 - 8, 2010

Abstract. *Satellite-based models for determining evapotranspiration (ET) are now routinely applied as part of water and water resources management operations of state and federal agencies. Strengths and weaknesses of more common models are briefly described. The more dependable and universal satellite-based models employ a surface energy balance (EB) where ET is computed as a residual of surface energy. This determination requires a thermal imager onboard the satellite, which is not common. The 'CIMEC' approach ("calibration using inverse modeling of extreme conditions") used by two moderate resolution, operational models is described where CIMEC calibrates around uncertainties and biases in satellite based energy balance components. Creating 'maps' of ET that are useful in management and in quantifying and managing water resources requires the computation of ET over monthly and longer periods such as growing seasons or annual periods. Interpolation between images from 'snapshot' models involves treatment of clouded areas of images, accounting for evaporation from wetting events occurring prior to or following overpass dates. A technique currently used in the METRIC model for accounting for evaporation from precipitation between images is described. How the interpolation is done substantially impacts the quality and accuracy of the final ET product.*

Keywords. Evapotranspiration, Remote Sensing, Landsat, Satellites, Energy Balance.

Introduction

Satellite-based models for determining evapotranspiration (ET) are now routinely applied as part of water and water resources management operations of state and federal agencies. They are also an integral component of research programs in land and climate processes. The very strong benefit of satellite-based models is the quantification of ET over large areas. This has enabled the estimation of ET from individual fields among populations of fields (Tasumi et al. 2005) and has greatly propelled field specific management of water systems and water rights as well as mitigation efforts under water scarcity. The more dependable and universal satellite-based models employ a surface energy balance (EB) where ET is computed as a residual of surface energy. This determination requires a thermal imager onboard the satellite, which is not common. We hope that more and more satellites will be equipped with moderately high resolution thermal imagers to provide greater opportunity to estimate spatial distributions of actual ET that are enormously valuable for monitoring effects of water shortage, water transfer, irrigation performance, and even impacts of crop type and variety and irrigation type on ET. Allen (2010b) showed that the current 16-day overpass return time of a single Landsat satellite is often insufficient to produce annual ET products due to impacts of clouds. An analysis of a 25 year record of Landsat imagery in southern Idaho showed the likelihood of producing annual ET products for any given year to increase by a factor of NINE times (from 5% probability to 45% probability) when two Landsat systems were in operation rather than one (Allen 2010b).

Satellite-based ET products are now being used in water transfers, to enforce water regulations, to improve development and calibration of ground-water models, where ET is a needed input for estimating recharge, to manage streamflow for endangered species management, to estimate water consumption by invasive riparian and desert species, to estimate ground-water consumption from at-risk aquifers, for quantification of native American water rights, to assess impacts of land-use change on wetland health, and to monitor changes in water consumption as agricultural land is transformed into residential uses (Bastiaanssen et al., 2005, Allen et al., 2005, Allen et al. 2007b).

The more widely used and operational remote sensing models tend to use a 'CIMEC' approach ("calibration using inverse modeling of extreme conditions") to calibrate around uncertainties and biases in satellite based energy balance components. Biases in EB components can be substantial, and include bias in atmospheric transmissivity, absolute surface temperature, estimated aerodynamic temperature, surface albedo, aerodynamic roughness, and air temperature fields. Current CIMEC models include SEBAL (Bastiaanssen et al. 1998a, 2005), METRIC (Allen et al., 2007) and SEBI-SEBS (Su 2002) and the process frees these models from systematic bias in the surface temperature and surface reflectance retrievals. Other models, such as the TSEB model (Kustas and Norman 1996), use absolute temperature and assumed air temperature fields, and so can be more susceptible to biases in these fields, and often require multiple times per day imagery. Consequently, coarser resolution satellites must be used where downscaling using finer resolution reflectance information is required.

Creating ‘maps’ of ET that are useful in management and in quantifying and managing water resources requires the computation of ET over monthly and longer periods such as growing seasons or annual periods. Successful creation of an ET ‘snapshot’ on a satellite overpass day is only part of the required process. At least half the total effort in producing a quantitative ET product involves the interpolation (or extrapolation) of ET information between image dates. This interpolation involves treatment of clouded areas of images, accounting for evaporation from wetting events occurring prior to or following overpass dates, and applying a grid of daily reference ET with the relative ET computed for an image, or a direct Penman-Monteith type of calculation, over the image domain for periods between images to account for day to day

variation in weather. The particular methodology for estimating these spatial variables substantially impacts the quality and accuracy of the final ET product.

Model Overview

Satellite based models can be separated into the following classes, building on Kalma et al. (2008):

- Surface Energy Balance
    - Full energy balance for the satellite image: $\lambda E = R_n - G - H$
    - Water stress index based on surface temperature and vegetation amounts
    - Application of a continuous Land Surface Model (LSM) that is partly initialized and advanced, in time, using satellite imagery
- Statistical methods using differences between surface and air temperature
- Simplified correlations or relationships between surface temperature extremes in an image and endpoints of anticipated ET
- Vegetation-based relative ET that is multiplied by a weather-based reference ET

where λE is latent heat flux density, representing the energy 'consumed' by the evaporation of water, R_n is net radiation flux density, G is ground heat flux density and H is sensible heat flux density to the air.

Except for the LSM applications, none of the listed energy balance methods, in and of themselves, go beyond the creation of a 'snapshot' of ET for the specific satellite image date. Large periods of time exist between snapshots when evaporative demands and water availability (from wetting events) cause ET to vary widely, necessitating the coupling of hydrologically based surface process models to fill in the gaps. The surface process models employed in between satellite image dates can be as simple as a daily soil-surface evaporation model based on a crop coefficient approach (for example, the FAO-56 model of Allen et al. 1998) or can involve more complex plant-air-water models such as SWAT (Arnold et al. 1994), SWAP (van Dam 2000), HYDRUS (Šimůnek et al. 2008), Daisy (Abrahamsen and Hansen 2000) etc. that are run on hourly to daily timesteps.

Problems with use of absolute surface temperature

Error in surface temperature (T_s) retrievals from many satellite systems can range from 3 – 5 K (Kalma et al. 2008) due to uncertainty in atmospheric attenuation and sourcing, surface emissivity, view angle, and shadowing. Hook and Prata (2001) suggested that finely tuned T_s retrievals from modern satellites could be as accurate as 0.5 K. Because near surface temperature gradients used in energy balance models are often on the order of only 1 to 5 K, even this amount of error, coupled with large uncertainties in the air temperature fields, makes the use of models based on differences in absolute estimates of surface and air temperature unwieldy.

Cleugh et al. (2007) summarized challenges in using near surface temperature gradients (dT) based on absolute estimates of T_s and air temperature, T_{air}, attributing uncertainties and biases to error in T_s and T_{air}, uncertainties in surface emissivity, differences between radiometrically derived T_s and the aerodynamically equivalent T_s required as a sourcing endpoint to dT.

The most critical factor in the physically based remote sensing algorithms is the solution of the equation for sensible heat flux density:

$$H = \rho_a \, c_p \, \frac{T_{aero} - T_a}{r_{ah}} \qquad (1)$$

where ρ_a is the density of air (kg m^{-3}), c_p is the specific heat of air (J kg^{-1} K^{-1}), r_{ah} is the aerodynamic resistance to heat transfer (s m^{-1}), T_{aero} is the surface aerodynamic temperature, and T_a is the air temperature either measured at standard screen height or the potential temperature in the mixed layer (K) (Brutsaert et al., 1993). The aerodynamic resistance to heat transfer is affected by wind speed, atmospheric stability, and surface roughness (Brutsaert, 1982). The simplicity of Eq. (1) is deceptive in that T_{aero} cannot be measured by remote sensing. Remote sensing techniques measure the radiometric surface temperature T_s which is not the same as the aerodynamic temperature. The two temperatures commonly differ by 1 to 5 °C, depending on canopy density and height, canopy dryness, wind speed, and sun angle (Kustas et al., 1994, Qualls and Brutsaert, 1996, Qualls and Hopson, 1998). Unfortunately, an uncertainty of 1 °C in $T_{aero} - T_a$ can result in a 50 W m^{-2} uncertainty in H (Campbell and Norman, 1998) which is approximately equivalent to an evaporation rate of 1 mm day^{-1}. Although many investigators have attempted to solve this problem by adjusting r_{ah} or by using an additional resistance term, no generally applicable method has been developed.

Campbell and Norman (1998) concluded that a practical method for using satellite surface temperature measurements should have at least three qualities: (i) accommodate the difference between aerodynamic temperature and radiometric surface temperature, (ii) not require measurement of near-surface air temperature, and (iii) rely more on differences in surface temperature over time or space rather than absolute surface temperatures to minimize the influence of atmospheric corrections and uncertainties in surface emissivity.

CIMEC Models (SEBAL and METRIC)

The SEBAL and METRIC models employ a similar inverse calibration process that meets these three requirements with limited use of ground-based data (Bastiaanssen et al., 1998a,b, Allen et al., 2007a). These models overcome the problem of inferring T_{aero} from T_s and the need for near-surface air temperature measurements by directly estimating the temperature difference between two near surface air temperatures, T_1 and T_2, assigned to two arbitrary levels z_1 and z_2 without having to explicitly solve for absolute aerodynamic or air temperature at any given height. The establishment of the temperature difference is done via inversion of the function for H at two known evaporative conditions in the model using the CIMIC technique. The temperature difference for a dry or nearly dry condition, represented by a bare, dry soil surface is obtained via $H=R_n - G - \lambda E$ (Bastiaanssen et al., 1998a):

$$T_1 - T_2 = \Delta T_a = \frac{H r_{ah}}{\rho_a \, c_p} \qquad (2)$$

At the other extreme, for a wet surface, essentially all available energy $R_n - G$ is used for evaporation λE. At that extreme, the classical SEBAL approach assumes that $H \approx 0$, in order to keep requirements for high quality ground data to a minimum, so that $\Delta T_a \approx 0$. Allen et al. (2001, 2007a) have used reference crop evapotranspiration, representing well-watered alfalfa, to represent λE for the cooler population of pixels in satellite images of irrigated fields in the METRIC approach, so as to better capture effects of regional advection of H and dry air, which can be substantial in irrigated desert. METRIC calculates $H = R_n - G - k_1 \lambda ET_r$ at these pixels, where ET_r is alfalfa reference ET computed at the image time using weather data from a local automated weather station, and ΔT_a from Eq. (2) , where $k_1 \sim 1.05$. In typical SEBAL and METRIC applications, z_1 and z_2 are taken as 0.1 and 2 m above the zero plane displacement

height (d). z_1 is taken as 0.1 m above the zero plane to insure that T_1 is established at a height that is generally greater than $d + z_{oh}$ (z_{oh} is roughness length for heat transfer). Aerodynamic resistance, r_{ah}, is computed for between z_1 and z_2 and does not require the inclusion and thus estimation of z_{oh}, but only z_{om}, the roughness length for momentum transfer that is normally estimated from vegetation indices and land cover type. H is then calculated in the SEBAL and METRIC CIMEC-based models as:

$$H = \rho_a c_p \frac{\Delta T_a}{r_{ah_{1-2}}} \quad (3)$$

One can argue that the establishment of ΔT_a over a vertical distance that is elevated above $d + z_{oh}$ (places the r_{ah} and established ΔT_a in a blended boundary layer that combines influences of sparse vegetation and exposed soil, thereby reducing the need for two source modeling.

Evaporative cooling creates a landscape having high ΔT_a associated with high H and high radiometric temperature and low ΔT_a with low H and low radiometric temperature. For example, moist irrigated fields and riparian systems have much lower ΔT_a and much lower T_s than dry rangelands. Allen et al. (2007a) argued, and field measurements in Egypt and Niger (Bastiaanssen et al., 1998b), China (Wang et al., 1998), USA (Franks and Beven, 1997), and Kenya (Farah, 2001) have shown the relationship between T_s and ΔT_a to be highly linear between the two calibration points

$$\Delta T_a = c_1 T_s - c_2 \quad (4)$$

where c_1 and c_2 are empirical coefficients valid for one particular moment (the time and date of an image) and landscape. By using the minimum and maximum values for ΔT_a as calculated for the nearly wettest and driest (i.e., coldest and warmest) pixel(s), the extremes of H are used, in the CIMEC process to find coefficients c_1 and c_2. The empirical Eq. (4) meets the third quality stated by Campbell and Norman (1998) that one should rely on differences in radiometric surface temperature over space rather than absolute surface temperatures to minimize the influence of atmospheric corrections and uncertainties in surface emissivity.

Equation (3) has two unknowns: ΔT_a and the aerodynamic resistance to heat transfer r_{ah} between the z_1 and z_2 heights which is affected by wind speed, atmospheric stability, and surface roughness (Brutsaert, 1982). Several algorithms take one or more field measurements of wind speed and consider these as spatially constant over representative parts of the landscape (e.g. Hall et al., 1992; Kalma and Jupp, 1990; Rosema, 1990). This assumption is only valid for uniform homogeneous surfaces. For heterogeneous landscapes a unique wind speed near the ground surface is required for each pixel. One way to meet this requirement is to consider the wind speed spatially constant at a blending height about 200 m above ground level, where wind speed is presumed to not be substantially affected by local surface heterogeneities. The wind speed at blending height is predicted by upward extrapolation of near-surface wind speed measured at an automated weather station using a logarithmic wind profile. The wind speed at each pixel is obtained by a similar downward extrapolation using estimated surface momentum roughness z_{0m} determined for each pixel.

Allen et al. (2007a) have noted that the inverted value for ΔT_a is highly tied to the value used for wind speed in its CIMEC determination. Therefore, they cautioned against the use of a spatial wind speed field at some blending height across an image with a single ΔT_a function. The application of the image-specific ΔT_a function with a blending height wind speed in a distant part of the image that is, for example, double that of the wind used to determine coefficients c_1 and

c_2 can estimate higher H than is possible based on energy availability. Gowda et al., (2008) presented a summary of remote sensing based energy balance algorithms for mapping ET that complements that by Kalma et al. (2008).

The SEBI-SEBS Model

The SEBS model was developed by (Su, 2002), building on the SEBI concept of Menenti and Choudhury (1993). SEBS establishes theoretical wet and dry boundary conditions in a type of CIMEC process to estimate H under these conditions using the Penman-Monteith ET equation (Monteith, 1981). For the dry condition, H is set to the R_n - G assuming ET to be zero and H at the wet condition is calculated by inserting a zero or nearly zero bulk surface resistance into the PM equation. Theoretical surface temperatures associated with these extremes are determined by extrapolating T and vapor pressure from some blending height to the surface under each flux condition, and at each pixel. Potential weaknesses in the SEBI-SEBS approach are the neglect of heat and vapor flux absorption by the near surface boundary layer along the temperature and vapor profiles when extrapolating to and from the blending layer. This causes flux divergence. This may result in an overstatement of the surface temperature for the dry condition. Another potential weakness is differences between estimated theoretical T_s and the T_s retrieved from the satellite, creating a bias that needs to be corrected empirically.

The TSEB Model

The Two Source Energy Balance (TSEB) model attempts to calculate the energy balance and aerodynamic fluxes of exposed soil and vegetation components separately. The model was derived by Norman et al. (1995) and Kustas and Norman (1996) based on a multilayer approach developed by Shuttleworth and Guerney (1990). This methodology generally requires some parameterizations governing the partitioning of composite radiometric surface temperature into soil and vegetation components, turbulent exchange of mass and energy at the soil level, and coupling/decoupling of energy exchange between vegetation and substrate (i.e., parallel or series resistance networks). Sensible heat fluxes are estimated by a temperature gradient-resistance system. Radiometric temperatures, resistances, sensible heat fluxes, and latent heat fluxes of the canopy and soil components are derived by iterative procedures (Gowda et al. 2008). Initial estimates of ET by the vegetation component are assigned values based on the Priestley-Taylor equation, which can underestimate ET by 50% in arid climates. The assigned value is sometimes refined in TSEB if required to balance the bulk T_s retrieval.

The SSEB Model

Senay et al. (2007) developed the Simplified Surface Energy Balance (SSEB) model that omitted the three components of the EB (R_n, H, G) and essentially scales relative reference ET, ET_rF, to surface temperature. Thus, there is little 'energy balance' remaining. While T_s does constitute the most fundamental relationship with ET_rF, the omission of impacts of albedo, aerodynamic roughness and ground heat flux may create sufficient error and bias in estimates to preclude the use where serious quantification of ET is needed. The SSEB approach still requires the use of near extreme values of T_s in an image during calibration.

Reflectance based ET methods

Reflectance based ET methods typically estimate relative fractions of reference ET (ET_rF, synonymous with the crop coefficient) based on some sort of vegetation index, for example, the normalized difference vegetation index, NDVI, and multiply the ET_rF by daily computed reference ET_r (Groeneveld et al., 2007). NDVI approaches don't directly or indirectly account for evaporation from soil, so they have difficulty in estimating evaporation associated with both

irrigation and precipitation wetting events, unless operated with a daily evaporation process model. The VI-based methods are therefore largely blind to the treatment of both irrigation and precipitation events, except on an average basis. In contrast, thermally based models detect the presence of evaporation from soil, during the snapshot, at least, via evaporative cooling. VI-based methods also do not pick up on acute water stress caused by drought or lack of irrigation, which is often a primary reason for quantifying ET. These models can be run with a background daily evaporation process model, similar to the EB-based models, to estimate evaporation from precipitation between satellite overpass dates.

Challenges with Snapshot models

The SEBAL, METRIC, SEBI-SEBS, TSEB and SSEB models, that can be applied at the relatively high spatial resolution of Landsat and similar satellites, despite their different relative strengths and weaknesses, all suffer from the inability to capture evaporation signals from episodic precipitation and irrigation events occurring between overpass dates. In the case of irrigation events, which are typically unknown to the processer in terms of timing and location, the random nature of these events in time can be somewhat accommodated via the use of multiple overpass dates during the irrigation season (Allen et al. 2007a). In this manner, the ET retrieval for a specific field may be biased high when the overpass follows an irrigation event, but may be biased low when the overpass just precedes an irrigation event. Allen et al. (2007a) suggested that monthly overpass dates over a seven month growing season, for example, can largely compensate for the impact of irrigation wetting on individual fields, especially when it is total growing season ET that is of most interest. The variance of the error in ET estimate caused by unknown irrigation events should tend to decrease with the square root of the number of images processed during the irrigation season.

The impact by precipitation events is a larger problem in converting the 'snapshot' ET images from energy balance models or other methods into monthly and longer period ET. Precipitation timing and magnitudes tend to be less random in time and have much larger variance in depth per wetting event than with irrigation. Because of this, the use of snapshot ET models to construct monthly and seasonal ET maps is more likely to be biased high (if a number of images happen to be 'wet' following a recent precipitation event) or low (if images happen to be 'dry', with precipitation occurring between images). The latter may often be the case since the most desired images for processing are cloud free.

One important use of ET maps is in the estimation of ground water recharge (Allen et al., 2007b). Ground water recharge is often uncertain due to uncertainty in both precipitation and ET, and is usually computed using the difference between P and ET, with adjustment for runoff. It is therefore important to maintain congruency between ET and P data sets or 'maps'. Lack of congruency can cause very large error in estimated recharge, especially in the more arid regions.

The LSM models, such as Noah (Chen et al., 2007) and MM5 are daily process models that utilize gridded precipitation and assimilated weather data to create gridded ET products usually based on a parameterized PM equation. Thermal information from satellite is not used in the energy balance, but rather reflectance information is used to update vegetation-based indices and surface albedo. These models are generally applied on large grids of 20 km or larger and are not able to distinguish ET from individual agricultural holdings or riparian systems. In addition, LSM models generally employ a Penman-Monteith equation to estimate ET where bulk surface conductance is estimated using satellite-based vegetation indices, with a soil-water balance used to dampen the potential ET estimate. Both the bulk surface conductance estimate and the amount of soil-water storage capacity estimate can have substantial uncertainty. The latter is impacted by knowledge of rooting depth and extent.

Adjusting for background evaporation

Often a Landsat or other image is processed on a date where antecedent rainfall has caused the evaporation from bare soil to exceed that for the surrounding monthly period. Often, for input to water balance applications, it is desirable that the final ET image represent the average evaporation conditions for the month. In that case, one approach is to adjust the 'background' evaporation of the processed image to better reflect that for the month or other period that it is to ultimately represent. This period may be a time period that is half way between other adjacent images.

An example of a sequence of Landsat images processed using the METRIC surface energy balance model for the south-western portion of the Nebraska Panhandle (Kjaersgaard and Allen, 2010) is shown in Figure 1 along with daily precipitation from the Scottsbluff High Plains Regional Climate Center (HPRCC) weather station. The August 13 image date was preceded by a wet period and followed by a very dry period, thus the evaporation from non-irrigated areas at the satellite image date is not representative for the month.

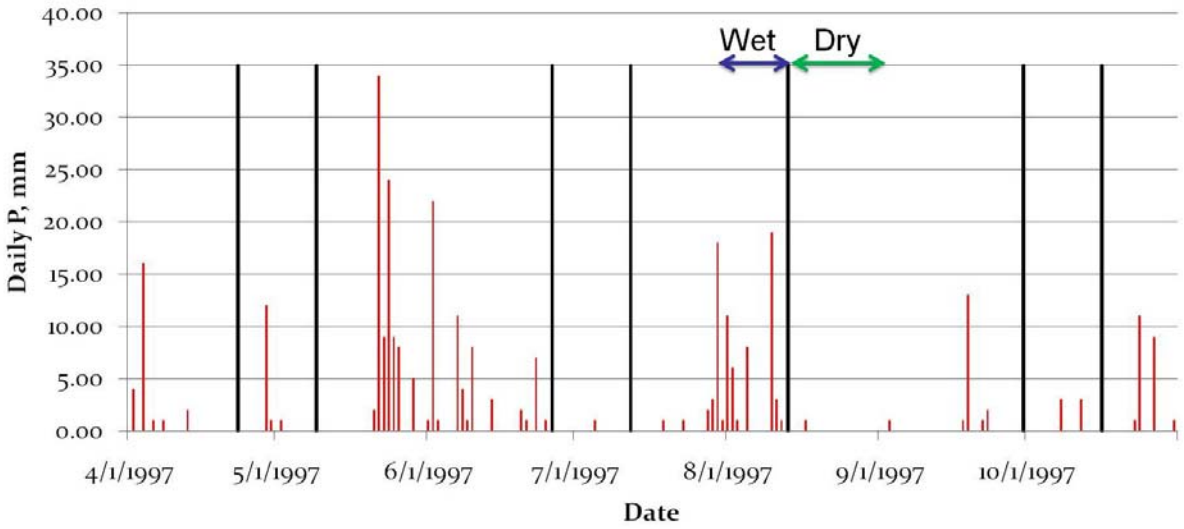

Figure 1. Image dates of nearly cloud free Landsat 5 path 33 row 31 images from the Nebraskan Panhandle in 1997 (black vertical bars) and precipitation recorded at the Scottsbluff HPRCC weather station (red bars). After Kjaersgaard and Allen (2010).

In making the adjustment for background evaporation, the background evaporation on the overpass date is subtracted out of the image and the average background evaporation is substituted in. Full adjustment is made for areas of completely bare soil, represented by NDVI = $NDVI_{bare\ soil}$, with no adjustment to areas having full ground covered by vegetation, represented by NDVI = $NDVI_{full\ cover}$, and with linear adjustment in between.

The following methodology is taken from a white paper developed by the University of Idaho during 2008 and 2009 (Allen 2008, rev. 2010). The ET_rF of the Landsat image is first adjusted to a 'basal' condition, where the evaporation estimate is free of rainfall induced evaporation, but still may contain any irrigation induced evaporation:

$$\left(ET_r F_i\right)_b = ET_r F_i - \left(ET_r F_{background}\right)_i \left(\frac{NDVI_{full\,cover} - NDVI_i}{NDVI_{full\,cover} - NDVI_{bare\,soil}} \right) \quad (5)$$

where $(ET_rF_{background})_i$ is the background evaporation on the image date (i) for bare soil, computed using a gridded FAO-56 two-stage evaporation model of Allen et al. (1998) with

modification to account for 'flash' evaporation from the soil skin (Allen 2010a) or some other soil evaporation model such as Hydrus or DAISY. The soil evaporation model is on a daily timestep using spatially distributed precipitation, reference ET, and soil properties. $(ET_rF_i)_b$ is the resulting 'basal' ET image for a particular image date, representing a condition having NDVI amount of vegetation and a relatively dry soil surface. This parameter represents the foundation for later adjustment to represent the longer period.

Adjustment for cases of Riparian vegetation

For riparian vegetation and similar systems, where soil water stress is not likely to occur due to the frequent presence of shallow ground water, an adjusted ET_rF is computed for the image date that reflects background evaporation averaged over the surrounding period in proportion to the amount of ground cover represented by NDVI:

$$\left(ET_rF_i\right)_{adjusted} = \left(ET_rF_i\right)_b + \left(\overline{ET_rF_{background}}\right)\left(\frac{NDVI_{full\,cover} - NDVI_i}{NDVI_{full\,cover} - NDVI_{bare\,soil}}\right) \quad (6)$$

where $\left(\overline{ET_rF_{background}}\right)$ is the average evaporation from bare soil due to precipitation over the averaging period (e.g., one month), calculated as:

$$\left(\overline{ET_rF_{background}}\right) = \frac{\sum_{1}^{n}\left(ET_rF_{background}\right)_i}{n} \quad (7)$$

Equations 5 and 6 can be combined as:

$$\left(ET_rF_i\right)_{adjusted} = ET_rF_i + \left(\left(\overline{ET_rF_{background}}\right) - \left(ET_rF_{background}\right)_i\right)\left(\frac{NDVI_{full\,cover} - NDVI_i}{NDVI_{full\,cover} - NDVI_{bare\,soil}}\right) \quad (8)$$

with limits $NDVI_{bare\ soil} \le NDVI_i \le NDVI_{full\ cover}$.

The outcome of this adjustment is to preserve any significant evaporation stemming from irrigation or ground-water and any transpiration stemming from vegetation, with adjustment only for evaporation stemming from precipitation to account for differences between the image date and that of the surrounding time period. In other words, if the initial ET_rF_i, prior to adjustment is high due to evaporation from irrigation or from high ground-water condition, much of that evaporation would remain in the adjusted ET_rF_i estimate.

Adjustments for Non-riparian vegetation

The following refinement to Eq. 8 is made for application to non-riparian vegetation, to account for those situations where, during long periods (i.e., months), soil moisture may have become limited enough that even transpiration of vegetation has been reduced due to moisture stress. If the Landsat image is processed during that period of moisture stress, then the ET_rF value for vegetated or partially vegetated areas will be lower than the potential (nonstressed) value. This can happen, for example, during early spring when winter wheat may go through stress prior to irrigation or a rainy period, or in desert and other dry systems.

This causes a problem in that the method of Eq. 8 attempts to 'preserve' the ET_rF of the vegetated portion of a pixel that was computed by METRIC on the image date. However, when a rain event occurs following the image date, not only will the ET_rF of exposed soil increase, but any stressed vegetation will equally 'recover' from moisture stress and the ET_rF of the vegetation fraction of the surface will increase. This situation may occur for rangeland and

dryland agricultural systems. It is therefore assumed that the ET_rF of nonstressed vegetation will be at least as high as the ET_rF of bare soil over the same time period, since it should have equal access to shallow water. An exception would be if the vegetation were sufficiently stressed to not recover transpiration potential. However, this amount of stress should be evidenced by a reduced NDVI. A minimum limit is therefore placed, using the background ET_rF $\left(\overline{ET_rF_{background}}\right)$ for the period.

To derive a modified Eq. 8, it is useful to first isolate the 'transpiration' portion of the ET_rF. On the satellite image date, the bulk ET_rF computed by METRIC for a pixel, is decomposed to:

$$ET_rF_i = (1 - f_c)\left(ET_rF_{background}\right)_i + f_c\left(ET_rF_{transpiration}\right)_i \quad (9)$$

where $ET_rF_{transpiration}$ is the apparent transpiration from the fraction of ground covered by vegetation, f_c. The f_c is estimated as $1 - f_s$, where f_s is the fraction of bare soil, and for consistency with equations 8, f_s is estimated as:

$$f_s = \left(\frac{NDVI_{full\,cover} - NDVI_i}{NDVI_{full\,cover} - NDVI_{bare\,soil}}\right) \quad (10a)$$

so that:

$$f_c = 1 - \left(\frac{NDVI_{full\,cover} - NDVI_i}{NDVI_{full\,cover} - NDVI_{bare\,soil}}\right) \quad (10b)$$

Eq. 9 is not used as is, since ET_rF_i comes from the energy balance-based ET image (i.e., from METRIC, etc.). However, one can rearrange Eq. 9 to solve for $ET_rF_{transpiration}$:

$$f_c\left(ET_rF_{transpiration}\right)_i = ET_rF_i - (1 - f_c)\left(ET_rF_{background}\right)_i \quad (11)$$

Now, if $ET_rF_{transpiration}$ is limited to the maximum of the $ET_rF_{transpiration}$ on the day of the image, or the $\left(\overline{ET_rF_{background}}\right)$ for the period, then:

$$\left(ET_rF_{transpiration}\right)_{adjusted} = \max\left[\left(ET_rF_{transpiration}\right)_i, \left(\overline{ET_rF_{background}}\right)\right] \quad (12)$$

Then the new ET_rF adjusted value becomes:

$$\left(ET_rF_i\right)_{adjusted} = (1 - f_c)\left(\overline{ET_rF_{background}}\right) + f_c\left(ET_rF_{transpiration}\right)_{adjusted}$$

or (13)

$$\left(ET_rF_i\right)_{adjusted} = (1 - f_c)\left(\overline{ET_rF_{background}}\right) + f_c \max\left[\left(ET_rF_{transpiration}\right)_i, \left(\overline{ET_rF_{background}}\right)\right]$$

where $\left(\overline{ET_rF_{background}}\right)$ is the average evaporation from bare soil due to precipitation over the averaging period (e.g., one month) and $ET_rF_{transpiration}$ is the original transpiration computed from Eq. 11. Eq. 11 and 13 can be combined so that:

$$\left(ET_rF_i\right)_{adjusted} = (1 - f_c)\left(\overline{ET_rF_{background}}\right) + \max\left[\left(ET_rF_i - (1 - f_c)\left(ET_rF_{background}\right)_i\right)_i, f_c\left(\overline{ET_rF_{background}}\right)\right] \quad (14)$$

Only areas with bare soil or partial vegetation cover are adjusted. Pixels having full vegetation cover, defined as when NDVI > 0.75, are not adjusted. An example of an image date where the adjustment increased the ET_rF for bare soil and partially vegetated areas is shown in Figure 2.

Figure 3 shows an example of an image date where the ET_rF from bare soil and partial vegetation cover was decreased by the adjustment.

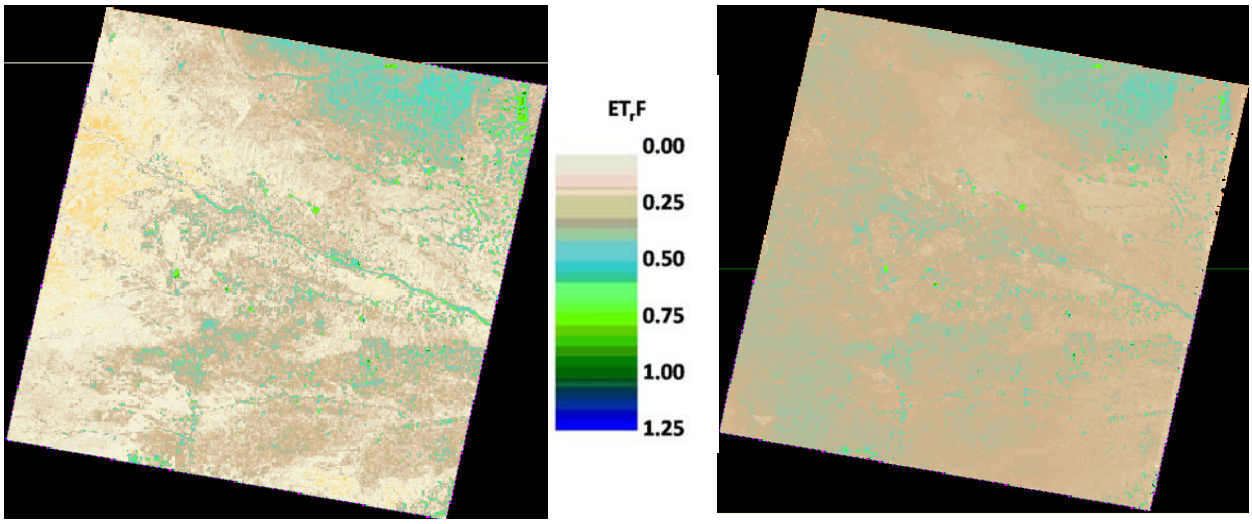

Figure 2. ET_rF in western Nebraska from May 9 1997 before (left) and after (right) adjustment for background evaporation representing the time period (~month) represented by that image. After Kjaersgaard and Allen (2010).

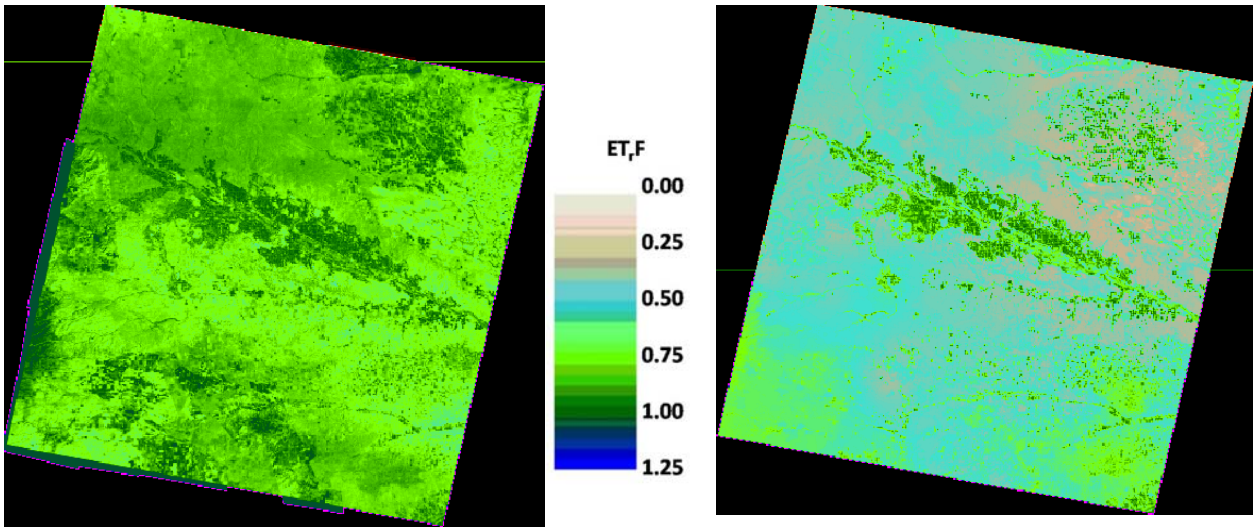

Figure 3. ETrF in western Nebraska on August 13 1997 before (left) and after (right) adjustment to reflect soil evaporation occurring over the time period (~ 1 month) represented by that image. Note that irrigated fields with full vegetation cover having a substantial transpiration component were not affected by the adjustment. After Kjaersgaard and Allen (2010).

Average ET_rF on image dates before and after adjustment for background evaporation is shown in Figure 4 from ten rangeland locations in western Nebraska. For some image dates, such as early and late in the season, the adjusted ET_rF values are “wetter” than that represented by the original image. Similarly, for other images dates, such as in the middle of the growing season, the images were “drier”. The adjustment for one image in August reduced the estimated ET for the month of August by nearly 50%, which is considerable.

It is noted, that the images no longer represent the ET from the satellite overpass dates after the adjustment for background evaporation. The images are merely an intermediate product that is

used as the input into an interpolation procedure when producing ET estimates for monthly or longer time periods.

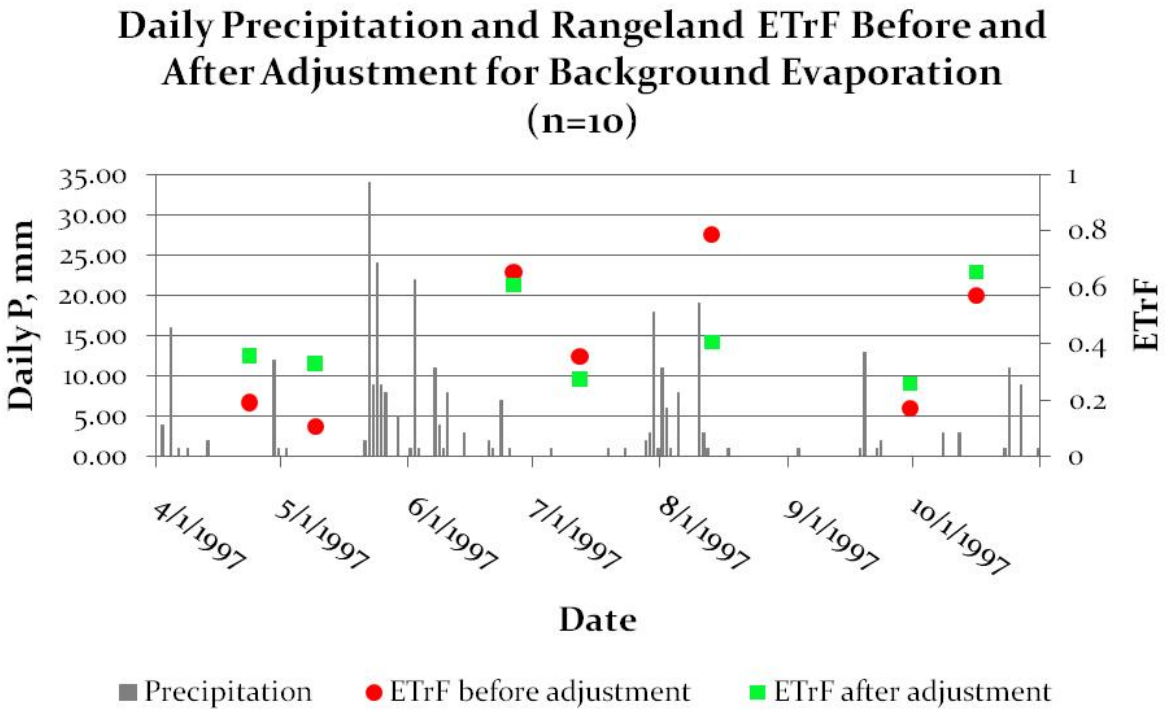

Figure 4. Average ET_rF from ten rangeland locations in western Nebraska before and after adjustment. Also shown is the precipitation from the Scottsbluff HPRCC weather station (after Kjaersgaard and Allen 2010).

Splining ET_rF between image dates

Energy balance based 'snapshot' models are used to create monthly and seasonal ET_rF and ET images based either on splining ET_rF between images and multiplying the ET_rF by daily ET_r on each day and then summing, or by applying an ET process model, such as the PM equation on a daily basis for each pixel of an image where the PM parameters are updated each new snapshot. The interpolation of ET_rF is simpler and is described here. Applications of METRIC have used a cubic spline interpolation procedure for ET_rF for more accurate interpolation for each day between images and to simulate curvilinear trends in vegetation development more closely, as shown in Figure 5.

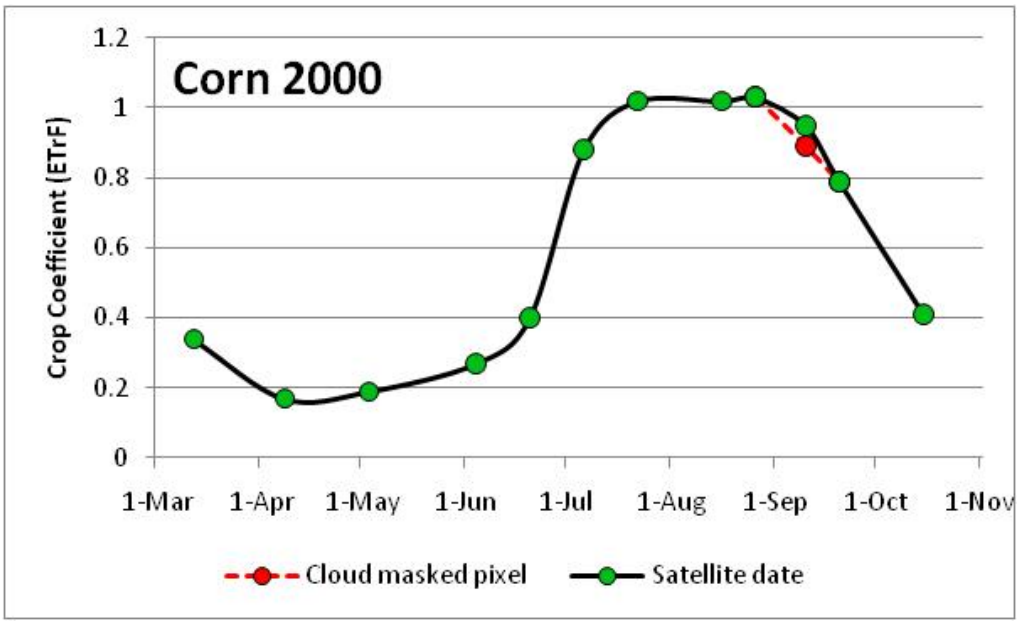

Figure 5. Schematic representation of the linear cloud gap filling and the cubic spline used to interpolate between image dates for a corn crop. The green points represent image dates and the black line is the splined interpolation between points; the red point represents the value of ET_rF that is interpolated linearly from the two adjacent image dates had the field had cloud cover on September 10.

Dealing with clouded parts of images

Satellite images often have clouds in portions of the images. ET_rF cannot be directly estimated for these areas using surface energy balance because cloud temperature masks surface temperature and cloud albedo masks surface albedo. Generally ET_rF for clouded areas must be filled in before application of further integration processes so that those processes can be uniformly applied to an entire image. The alternative is to directly interpolate ET_rF between adjacent (in time) image dates or to run some type of daily ET process model that is based on gridded weather data.

In METRIC applications (Allen et al. 2007b), ET_rF for clouded areas of images is usually filled in prior to interpolating ET_rF for days between image dates (and multiplying by gridded ET_r for each day to obtain daily ET images). A linear interpolation, as shown in Figure 5, is used to fill in ET_rF for clouded portions of images rather than curvilinear interpolation that is used to interpolate ET_rF between nonclouded image portions because some periods between cloud-free pixel locations can be as long as several months. Often, the change in crop vegetation amount and thus ET_rF is uncertain during that period. Thus, the use of curvilinear interpolation can become speculative.

Image processing code can be created to conduct the 'filling' of cloud masked portions of images. The code used with METRIC accommodates up to eight image dates and corresponding ET_rF, with conditionals used to select the appropriate set of images to interpolate between, depending on the number of consecutive images that happen to be cloud masked for any specific location. Missing (clouded) ET_rF for end-member images (those at the start or end of the growing season) must be estimated by extrapolation of the nearest (in time) image having valid ET_rF, or alternatively, for end-member images, a 'synthetic' image can be created, based on daily soil water balance or other methods, to be used to substitute for cloud-masked areas. Often, the availability of images for early spring is limited due to clouds. In these cases, the

ET_rF values in the synthetic image are based on a soil-water balance–weather data model, such as the FAO-56 evaporation model or Hydrus or DAISY, applied over the month of April, for example, to provide an improved estimate of ET_rF over the early season. The synthetic image(s) are strategically placed, date-wise, so that the cloud-filling process and the subsequent cubic spline process used to interpolate final ET_rF has end-points early enough in the year to provide ET_rF for all days of interest during the growing period.

Examples of cloud masking for a METRIC application in western Nebraska are shown in Figure 6. Black portions within each image are the areas masked for clouds. ET_rF for cloud masked areas was filled in for individual Landsat dates prior to splining ET_rF between images. The cloud mask gap filling and interpolation of ET between image dates entails interpolating the ET_rF for the missing area from the previous and following images that have ET_rF for that location.

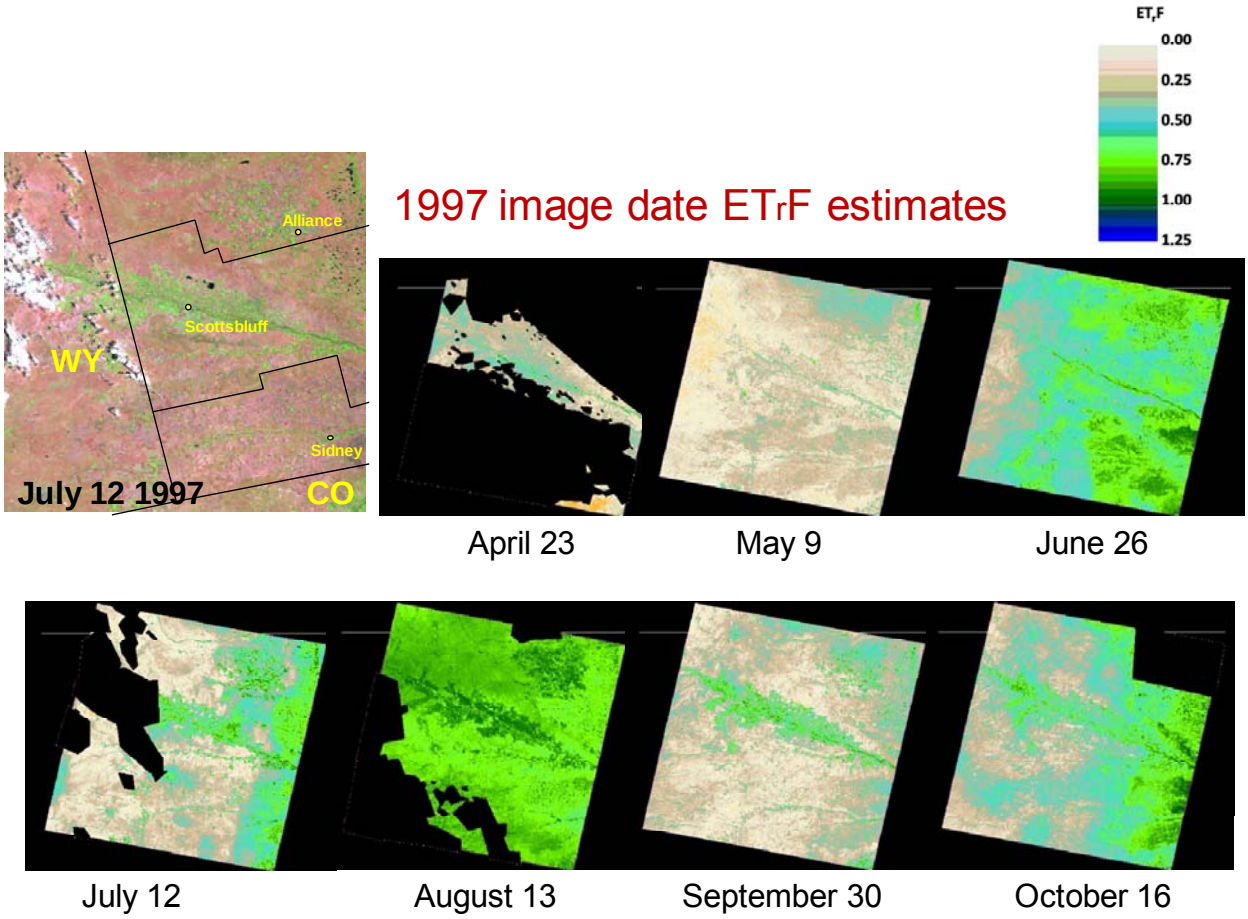

Figure 6. Maps of cloud masked ET_rF from seven 1997 images dates. The geographical extent of the North Platte and South Platte Natural Resource Districts boundaries and principal cities is shown on the image in the top left corner (after Kjaersgaard and Allen 2010).

In current METRIC applications, gaps in the ET_rF maps occurring as a result of the cloud masking are filled in using linear time-weighted interpolation of ET_rF values from the previous image and the nearest following satellite image date having a valid ET_rF estimate, adjusted for vegetation development. The NDVI is used to indicate change in vegetation amount from one image date to the next. The principle is sketched in Figure 7, where a location in the two nearest images (i-1 and i+1) happen to be clouded. During the gap filling, the interpolated values for the

clouded and cloud-shadowed areas are adjusted for differences in residual soil moisture between the image dates occurring as a result of heterogeneities in precipitation (such as by local summer showers) in inverse proportion to NDVI and by adding an interpolated 'basal' ET_rF from the previous and following satellite image dates. This procedure is needed to remove artifacts of this precipitation-derived evapotranspiration that are unique to specific image dates but that may not be representative of the image date that is to be represented by the ET_rF from the previous and the following images. A comparison between cloud gap filling without and with adjustment for background evaporation is shown in Figure 8.

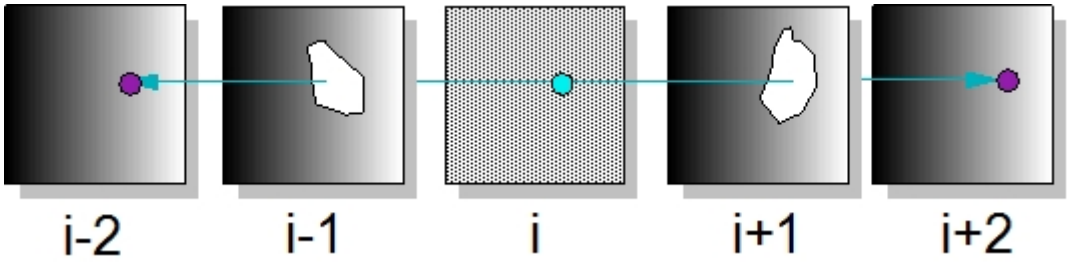

Figure 7. Principle of cloud gap filling. "i" is the image having cloud masked areas to be filled; "i-1" and "i-2" are the two earlier images than image I; "i+1" and "i+2" are the two following images.

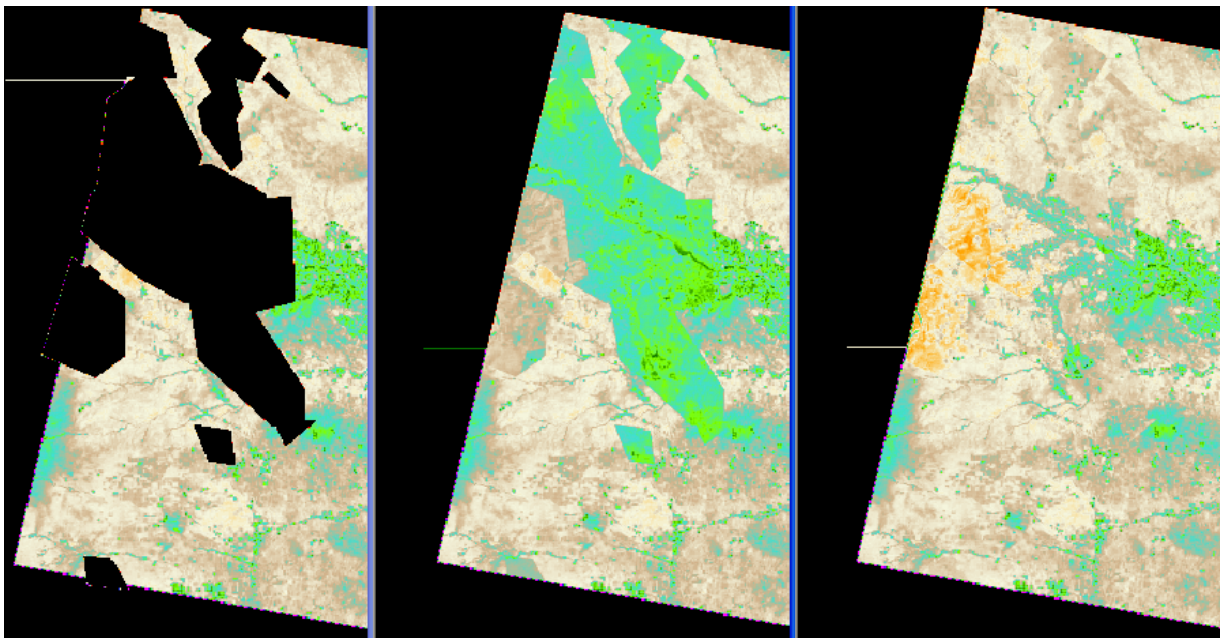

Figure 8. Maps of ET_rF from Landsat 5, July 12 1997, in western Nebraska after cloud masking (left) (black indicate areas removed during cloud masking or background); and after cloud gap filling without (center) and with (right) adjustment for vegetation amount and background evaporation from antecedent rainfall. The August 13 image from which part of the ET_rF data was borrowed was quite wet from precipitation, and thus had high ET_rF for low-vegetated areas, and therefore created substantially overestimated ET_rF for July 12 in the filled areas (center). After Kjaersgaard and Allen (2010).

Other remaining challenges with operational models for spatial ET

In addition to challenges in producing daily time series of spatial ET, as described in the previous section, other challenges remaining with all models, snapshot and process models alike include the following. A number of these were further described in Allen et al. (2010),

including estimation of aerodynamic roughness at 30 m scale; aerodynamic roughness and wind speed variation in complex terrain and in tall, narrow vegetation systems such as riparian systems; and estimation of hemispherical reflectance from bi-direction reflectance in deep vegetation canopies from nadir-looking satellites such as Landsat. Other remaining challenges include estimation of soil heat and aerodynamic sensible heat fluxes in sparse desert systems and in playa and estimation of ET over 24-hour periods using one-time of day observation (for example ~1000 solar time for Landsat) based on energy balance, especially where substantial stomatal control exists (desert and forest). METRIC capitalizes on using weather-based reference ET to make this transfer over time, which has been shown to work well for irrigated crops, especially in advective environments (Allen et al. 2007a). However, the evaporative fraction, as used in early SEBAL (Bastiaanssen et al. 1998a) and other models may perform best for rainfed systems where, by definition, advection can not exist. Therefore, a mixture of ET_rF and EF may be optimal, based on land-use class.

Conclusions

Satellite-based models for determining evapotranspiration (ET) are now routinely applied as part of water and water resources management operations of state and federal agencies. The very strong benefit of satellite-based models is the quantification of ET over large areas. Strengths and weaknesses of common EB models often dictate their use. The more widely used and operational remote sensing models tend to use a 'CIMEC' approach ("calibration using inverse modeling of extreme conditions") to calibrate around uncertainties and biases in satellite based energy balance components. Creating ‘maps’ of ET that are useful in management and in quantifying and managing water resources requires the computation of ET over monthly and longer periods such as growing seasons or annual periods. This requires accounting for increases in ET from precipitation events in between images. An approach for estimating the impacts on ET from wetting events in between images has been described. This method is empirical and can be improved in the future with more complex, surface conductance types of process models, such as used in Land surface models (LSM’s). Interpolation processes involve treatment of clouded areas of images, accounting for evaporation from wetting events occurring prior to or following overpass dates, and applying a grid of daily reference ET with the relative ET computed for an image, or a direct Penman-Monteith type of calculation. These approaches constitute a big step forward in computing seasonal ET over large areas with relatively high spatial (field-scale) definition, where impacts of intervening wetting events and cloud occurrence are addressed.

References

Abrahamsen, P. and S. Hansen . 2000. Daisy: an open soil-crop-atmosphere system model. *Environmental Modelling and Software,* 15(3):313-330.

Allen, R.G. 2008, rev. 2010. Procedures for adjusting METRIC-derived ETrF Images for Background Evaporation from Precipitation Events prior to Cloudfilling and Interpretation of ET between Image Dates. Internal memo., University of Idaho. 11 pages. Version 7, last revised April 2010.

Allen, R.G., 2010a. Modification to the FAO-56 Soil Surface Evaporation Algorithm to Account for Skin Evaporation during Small Precipitation Events. Memorandum prepared for the UI Remote Sensing Group, revised May 16, 2010, August 2010, 9 pages.

Allen, R.G. 2010b. Assessment of the probability of being able to produce Landsat resolution images of annual (or growing season) evapotranspiration in southern Idaho – and effect of the number of satellites. Memorandum prepared for the Landsat Science Team. 5 p.

Allen, R. G., Pereira, L., Raes, D., and Smith, M. 1998. *Crop Evapotranspiration*, Food and Agriculture Organization of the United Nations, Rome, It. ISBN 92-5-104219-5. 300 p.

Allen, R.G., W.B.M. Bastiaanssen, M. Tasumi, and A. Morse. 2001. Evapotranspiration on the watershed scale using the SEBAL model and LandSat Images. Paper Number 01-2224, ASAE, Annual International Meeting, Sacramento, California, July 30-August 1, 2001.

Allen, R.G., M.Tasumi, A.T. Morse, and R. Trezza. 2005. A Landsat-based Energy Balance and Evapotranspiration Model in Western US Water Rights Regulation and Planning. *J. Irrigation and Drainage Systems.* 19: 251-268.

Allen, R.G., M. Tasumi and R. Trezza. 2007a. Satellite-based energy balance for mapping evapotranspiration with internalized calibration (METRIC) – Model. ASCE *J. Irrigation and Drainage Engineering* 133(4):380-394.

Allen, R.G., M. Tasumi, A.T. Morse, R. Trezza, W. Kramber, I. Lorite and C.W. Robison. 2007b. Satellite-based energy balance for mapping evapotranspiration with internalized calibration (METRIC) – Applications. ASCE *J. Irrigation and Drainage Engineering* 133(4):395-406.

Allen,R.G., J. Kjaersgaard, R. Trezza, A. Oliveira, C. Robison, and I. Lorite-Torres. 2010. Refining components of a satellite based surface energy balance model to complex-land use systems. Proceedings of the Remote Sensing and Hydrology Symposium, Jackson Hole, Wyo, IAHS. Oct. 2010. 3 p.

Arnold, J.G., J.R. Williams, R. Srinivasan, K.W. King and R.H. Griggs. 1994. SWAT--Soil and Water Assessment Tool--User Manual. Agricultural Research Service, Grassland, Soil and Water Research Lab, US Department of Agriculture.

Bastiaanssen, W.G.M., M. Menenti, R.A. Feddes, and A.A. M. Holtslag. 1998a. A remote sensing surface energy balance algortithm for land (SEBAL). Part 1: Formulation. *J. of Hydrology* 198-212.

Bastiaanssen, W.G.M., H. Pelgrum, J. Wang, Y. Ma, J.F. Moreno, G.J. Roerink, R.A. Roebeling, and T. van der Wal. 1998b. A remote sensing surface energy balance algortithm for land (SEBAL). Part 2: Validation. *J. of Hydrology* 212-213: 213-229.

Bastiaanssen , W.G.M., E.J.M. Noordman , H. Pelgrum, G. Davids, B.P. Thoreson and R.G. Allen. 2005. SEBAL model with remotely sensed data to improve water resources management under actual field conditions. *J. Irrig. Drain. Engrg*, ASCE 131(1): 85-93.

Brutsaert, W. 1982. *Evaporation into the atmosphere*. Reidel, Dordrecht, The Netherlands.

Brutsaert, W., A.Y. Hsu, and T.J. Schmugge. 1993. Parameterization of surface heat fluxes above a forest with satellite thermal sensing and boundary layer soundings. *J. Appl. Met.* 32: 909-917.

Campbell, G.S. and J.M. Norman. 1998. *An introduction to environmental biophysics.* Sec. Edition. Springer, New York.

Chen, F., K.W. Manning, M.A.Lemone,S.B. Trier, J.G. Alfieri, R.Roberts, M. Tewari, D. Niyogi, T.W. Horst, S.P. Oncley, J.B. Basara, and P.D. Blanken. 2007. Description and Evaluation of the Characteristics of the NCAR High-Resolution Land Data Assimilation System. *J. Appl. Meteorol. and Climatol*. 46: 694-713.

Cleugh, H.A., R. Leuning, Q. Mu and S.W. Running. 2007. Regional evaporation estimates from flux tower and MODIS satellite data. *Remote Sens. Environ*. 106:285-304.

Farah, H.O. 2001. Estimation of regional evaporation under different weather conditions from satellite and meteorological data. A case study in the Naivasha Basin, Kenya. Doctoral Thesis Wageningen University and ITC.

Franks, S.W. and K.J. Beven. 1997. Estimation of evapotranspiration at the landscape scale: a fuzzy disaggregation approach. *Water Resour. Res*. 33:2929-2938.

Gowda, P.H., J.L. Chávez, P.D. Colaizzi, S.R. Evett, T.A. Howell, and J.A. Tolk. 2008. ET mapping for agricultural water management: present status and challenges. *Irrig. Sci.* 26:223-237

Groeneveld, D.P., W.J. baugh, J.S. Sanderson and D.J. Cooper. 2007. Annual groundwater evapotranspiration mapped from single satellite scenes. *J. Hydrol*. 344:146-156.

Hall, F.G., K.F. Huemmrich, S.J. Goetz, P.J. Sellers, and J.E. Nickeson. 1992. Satellite remote sensing of the surface energy balance: success, failures and unresolved issues in FIFE. *J. Geophys. Res*. 97(D17):19061-19090.

Hook, S. and A.J. Prata. 2001. Land surface termpature measured by ASTER-First results. *Geophys. Res. Abs*., 26th Gen. Assemb. 3:71.

Kalma, J.D. and D.L.B. Jupp. 1990. Estimating evaporation from pasture using infrared thermography: evaluation of a one-layer resistance model. *Agr. and Forest Met*. 51:223-246.

Kalma, J.D., T.R. McVicar, and M.F. McCabe. 2008. Estimating land surface evaporation: a review of methods using remotely sensed surface temperature data. *Surv. Geophys* 29:421-469.

Kjaersagaard, J. and R.G. Allen. 2010. Remote Sensing Technology to Produce Consumptive Water Use Maps for the Nebraska Panhandle. Final completion report submitted to the University of Nebraska. 60 pages.

Kustas, W. P., and J. M. Norman. 1996. Use of remote sensing for evapotranspiration monitoring over land surfaces. *Hydrol. Sci. J*. 41(4): 495-516.

Kustas, W. P., Moran, M. S., Humes, K. S., Stannard, D. I., Pinter, J., Hipps, L., and Goodrich, D. C. 1994. Surface energy balance estimates at local and regional scales using optical remote sensing from an aircraft platform and atmospheric data collected over semiarid rangelands. *Water Resources Research*, 30(5): 1241-1259.

Menenti, M., and B. J. Choudhury. 1993. Parameterization of land surface evapotranspiration using a location dependent potential evapotranspiration and surface temperature range. In Proc. Exchange Processes at the Land Surface for a Range of Space and Time Scales , 561-568. Bolle et al., eds. IAHS Publication 212. International Association of Hydrological Sciences.

Monteith, J. L. 1981. Evaporation and surface temperature. *Quarterly J. Royal Meteorological Soc.* 107(451): 1-27.

Norman, J. M., W. P. Kustas, and K. S. Humes. 1995. Source approach for estimating soil and vegetation energy fluxes from observations of directional radiometric surface temperature. *Agric. Forest Meteorology* 77(3-4): 263-293.

Qualls, R., and Brutsaert, W. (1996). “Effect of vegetation density on the parameterization of scalar roughness to estimate spatially distributed sensible heat fluxes.” *Water Resources Research*, 32(3): 645-652.

Qualls, R., and Hopson, T. (1998). “Combined use of vegetation density, friction velocity, and solar elevation to parameterize the scalar roughness for sensible heat.” *J. Atmospheric Sciences,* 55: 1198-1208.

Rosema, A. 1990. Comparison of meteosat-based rainfall and evapotranspiration mapping of Sahel region. *Rem. Sens. Env*. 46: 27-44.

Senay, G.B., M. Budde, J.P. Verdin and A.M. Melesse. 2007. A Coupled Remote Sensing and Simplified Surface Energy Balance Approach to Estimate Actual Evapotranspiration from Irrigated Fields. *Sensors* 7: 979-1000.

Shuttleworth, J., and R. Guerney. 1990. The theoretical relationship between foliage temperature and canopy resistance in sparse crops. *Quarterly J. Royal Meteorological Soc.* 116(492): 497-519.

Šimůnek, J., M.T. van Genuchten, and M. Šejna. 2008. Development and applications of the HYDRUS and STANMOD software packages and related codes. *Vadose Zone J.* 7:587-600.

Su, Z. 2002. The surface energy balance system (SEBS) for estimation of turbulent fluxes. *Hydrol. Earth Systems Sci.* 6(1): 85-99.

Tasumi, M., R. G. Allen, R. Trezza, J. L. Wright. 2005. Satellite-based energy balance to assess within-population variance of crop coefficient curves, *J. Irrig. and Drain. Engrg,* ASCE 131(1): 94-109.

Van Dam, J.C., 2000. Field-scale water flow and solute transport: SWAP model concepts, parameter estimation and case studies. Proefschrift Wageningen Universiteit.

Wang, J., W.G.M Bastiaanssen, Y. Ma, and H. Pelgrum. 1998. Aggregation of land surface parameters in the oasis-desert systems of Northwest China. *Hydr. Processes* 12:2133-2147.